

FABRICATION AND CHARACTERISATION OF SCALN-BASED PIEZOELECTRIC MEMS CANTILEVERS

P.M. Mayrhofer, E. Wistrela, M. Kucera, A. Bittner and U. Schmid

Institute of Sensor and Actuator Systems, Vienna University of Technology, 1040 Vienna, Austria.

ABSTRACT

Scandium (Sc) doping of aluminium nitride (AlN) increases the piezoelectric actuation potential due to substantially enhanced piezoelectric constants. This work demonstrates the fabrication of MEMS cantilevers actuated by sputter deposited $\text{Sc}_x\text{Al}_{1-x}\text{N}$ thin films ($x = 27\%$) sandwiched between gold electrodes. Patterning of $\text{Sc}_x\text{Al}_{1-x}\text{N}$ films is performed by a reactive ion etching process using SiCl_4 . The dynamic actuation potential of the fabricated devices is evaluated with Laser Doppler Vibrometry and with electrical impedance spectroscopy measurements. When applying the Butterworth Van-Dyke equivalent circuit a significant increase of the effective transverse piezoelectric constant d_{31} is demonstrated.

KEYWORDS

ScAlN thin films, piezoelectric, MEMS cantilever, impedance spectrum, Laser Doppler Vibrometer.

INTRODUCTION

Piezoelectric thin films are used within MEMS resonators for excitation and sensing purposes. Resonance frequency and damping (Q-factor) of cantilever type MEMS are sensitive e.g. to changes in a fluid environment, to mass or stress loading which can be employed for biosensing applications or measurement of liquid properties such as density (ρ) and viscosity (η) [1, 2]. For the latter purpose, aluminium nitride (AlN) has been successfully applied to all-electric MEMS resonators for Q-factor measurements as $Q \propto (\eta\rho)^{-1/2}$ [2]. The device performance, however, is improved by a higher piezoelectric modulus d_{31} as the conductance peak ΔG is proportional to d_{31}^2 [2]. Therefore, $\text{Sc}_x\text{Al}_{1-x}\text{N}$ offers great potential especially for such applications since the piezoelectric constants increase with Sc content x . The transverse piezoelectric coefficient d_{31} increases from $d_{31} \approx -2$ pm/V for $x = 0\%$ up to -13 pm/V for $x = 42\%$ [3]. Additionally, the elastic modulus decreases from $E_1 = 325$ GPa for pure AlN to $E_1 = 170$ GPa for $x = 42\%$. Once this concentration is exceeded a phase transition from wurtzite to cubic type crystal structure takes place, thus preventing further increase of the piezoelectric modulus. Reported MEMS device based on Sc doped AlN include surface as well as bulk acoustic wave devices [4-7]. But, released micromachined structures, such as cantilevers with $\text{Sc}_x\text{Al}_{1-x}\text{N}$ are not reported in literature. This work focuses on $\text{Sc}_x\text{Al}_{1-x}\text{N}$ with $x = 27\%$ as the piezoelectric active thin film on cantilever devices thereby, avoiding disadvantageous effects near the phase transition, but exploiting the high increase in d_{31} reported for this concentration [8]. Electrical characterisation is performed

based on a self-actuation self-sensing approach in addition to optical evaluation of the deflection applying Laser Doppler Vibrometry.

DEVICE FABRICATION

Work Flow

Piezoelectric cantilevers in different geometrical dimensions are fabricated, each one based on a $\text{Sc}_x\text{Al}_{1-x}\text{N}$ thin film sandwiched between two symmetric pairs of gold (Au) electrodes. The electrode pairs enable the individual excitation of out-of-plane as well as in-plane eigenmodes. The designs consider different cantilever dimensions to demonstrate the impact of electrode area on mechanical

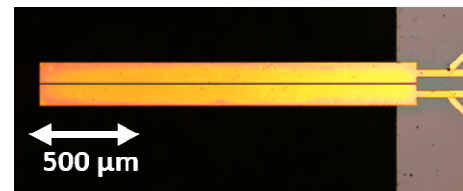


Figure 1: Optical micrograph of a typical MEMS cantilever device in top view.

deflection and the impedance characteristics. In Figure 1, a typical design of a released cantilever is shown. The top electrode pair is visible and $30\ \mu\text{m}$ wide feedlines for sensing and excitation. The fabrication process is based on $100\ \text{mm}$ SOI wafers with a device layer thickness of $t_b = 20\ \mu\text{m}$ and an additional bi-layer of $\text{SiO}_2/\text{Si}_x\text{N}_y$ ($150\ \text{nm}/80\ \text{nm}$) on top. The bottom Au electrode pair and

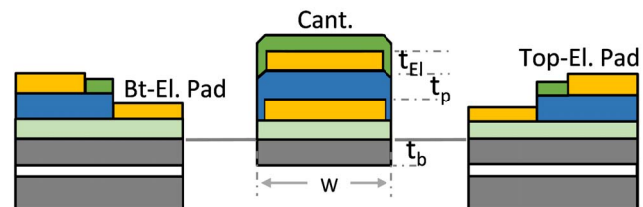


Figure 2: Schematic front view on the cantilever (Cant.) and the silicon frame including bonding pads for top (Top-El. pad) and bottom electrodes (Bt-El. pad). Stack sequence of cantilever structure and SOI wafer: Si_xN_y , Au ($t_{\text{El}}=400\ \text{nm}$), ScAlN ($t_p=500\ \text{nm}$), Au, SiO/SiN , Si ($t_b=20\ \mu\text{m}$), SiO - white.

the contact pads comprising a Cr adhesion layer are thermally evaporated on the nitride and patterned with optical lithography and a lift-off process. Subsequently, the piezoelectric $\text{Sc}_x\text{Al}_{1-x}\text{N}$ layer is deposited. A schematic front view of all layers associated with the cantilever is illustrated in Figure 2.

The $\text{Sc}_x\text{Al}_{1-x}\text{N}$ with $x = 27\%$ and thickness $t_p = 500\ \text{nm}$ is deposited via DC reactive magnetron sputtering from a

100 mm AlSc alloy target. The thin film is prepared in an Ar/N₂ atmosphere at nominally unheated substrate conditions. Au top electrodes are again thermally evaporated and patterned with a lift-off process. Reactively sputtered silicon nitride (Si_xN_y) is used as mask material for the patterning process of ScAlN and simultaneously acts as electrode passivation. Both films, ScAlN and Si_xN_y are dry etched by reactive ion etching (RIE), described in the following section. Both the device layer and the handle wafer are etched with a deep reactive ion etching (DRIE) process and finally, the cantilevers are released in hydrofluoric acid by removing the SiO₂. Finally, the devices are electrically connected to the DIP package with Au wires by thermal bonding.

Reactive ion etching of ScAlN

Compared to wet chemically etching patterning of thin films with an inductively coupled plasma reactive ion etching process (ICP-RIE) is advantageous due to its high anisotropic etch performance. This prevents underetching effects that may lead to an electrical short circuit of top and bottom electrode. For pure AlN thin films highest etch rates are reported in chloride based gas mixtures [9]. This work

The SiCl₄ process parameters were: pressure $p = 15$ mTorr, RF power: 225 W, ICP power: 150 W. The etch rate r decreases from $r = 24$ nm/min for pure AlN to $r = 10$ nm/min with a Sc concentration of $x = 27\%$. Due to the high etch rate of Si_xN_y in SiCl₄ (20 nm/min) the thickness compared to ScAlN needs to be larger than 2:1. Figure 3(a) shows the resulting steep sidewalls in an electron microscope (SEM) micrograph that illustrate the anisotropic character of the process. This preliminary test was performed with a chromium etch mask, having a higher selectivity to ScAlN than Si_xN_y. The thickness of the etched ScAlN thin film is 500 nm. In Figure 3(b), a SEM micrograph of a released cantilever structure is shown. In contrast to the device fabrication, the release of the structure in Figure 3(b) was performed in a xenon fluoride (XeF₂) based process to remove the Si device layer. In addition to ScAlN sidewalls, the Si_xN_y mask layer is shown in the picture. For this mask layer an initial thickness of 1600 nm was used to pattern a 750 nm thick ScAlN thin film. The thickness of the remaining Si_xN_y after the process is approximately 500 nm.

MEASUREMENT RESULTS

Cantilever Deflection

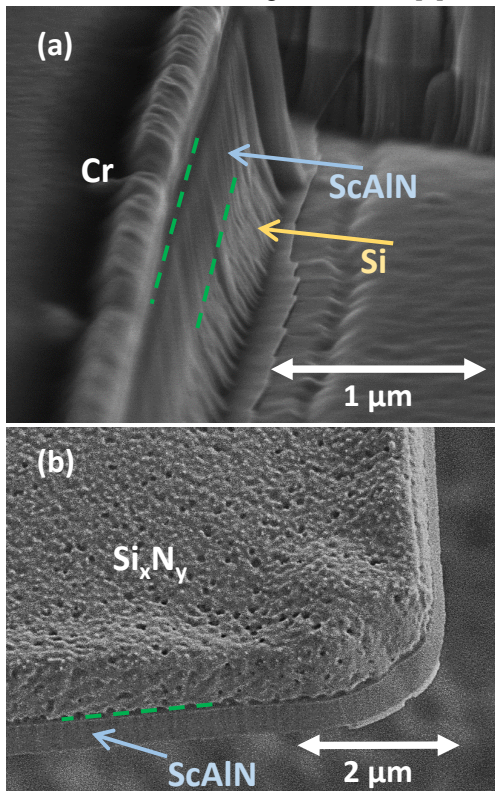


Figure 3: Scanning electron microscopy images of patterned ScAlN after SiCl₄ etching process. (a) Cr-hardmask / ScAlN / Si-substrate and (b) Si_xN_y hardmask / ScAlN - after release by XeF₂.

employs SiCl₄ for the ICP-RIE process to pattern ScAlN and pure AlN thin films with a RIE Oxford 100 system. Prior to the ScAlN etching process the Si_xN_y hardmask was patterned in the ICP system using a mixture of SF₆ and O₂.

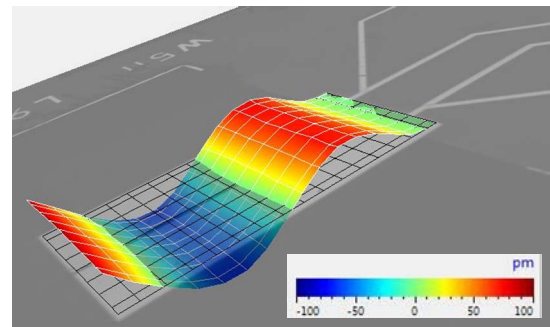


Figure 4: Z-Deflection of a cantilever excited in the 3rd OP Eigenmode measured with Laser Doppler Vibrometry

Initial characterization of the bonded cantilever is done optically employing a Laser Doppler Vibrometer (LDV) from Polytec (MSA 400). The study is focused on the analysis of out-of plane (OP) eigenmodes in air at ambient pressure. For that reason, an AC voltage amplitude of 0.5 V is applied to the top electrode pair while the bottom electrodes are grounded. Figure 4 shows the vertical deflection of a 511 x 959 μm² sized cantilever oscillating in the 3rd OP mode (496 kHz), whereas experimental data are gained from the matrix of points covering the cantilever surface. The LDV grid measurements are used to identify the mode type and order. For a further evaluation of the deflection a line scan is performed along the cantilever axis. The vertical deflection amplitude along this line is then used to extract an effective value for the transversal piezoelectric coefficient d_{31} . For that purpose, a theoretical model describing the cantilever deflection along the center line is fitted to the deflection data.

Table 1: Key parameters of ScAlN or AlN based cantilevers having different width W and length L . Measured resonance frequency f , calculated resonance frequency f_{th} , Q -factor and conductance peak ΔG from BVD equivalent circuit with parameters such as parallel resistance / capacitance R_p/C_p , motional resonance parameters R_m, L_m, C_m . Out-of plane resonance number num, effective piezoelectric constant d_{31} obtained from electrical conductance, $d_{31,V}$ from LDV based optical deflection measurements.

| Type | Num | W / μm | L / μm | f / kHz | f_T / kHz | Q | ΔG / μS | $\Delta G/Q$ / nS | d_{31} / pm/V | $d_{31,V}$ / pm/V | R_p / M Ω | C_p / pF | R_m / k Ω | L_m / H | C_m / fF |
|--------|-----|-------------------|-------------------|---------|-------------|-----|----------------------------|-------------------|-----------------|-------------------|--------------------|------------|--------------------|-----------|------------|
| ScAlN1 | 1 | 804 | 1203 | 18.2 | 18.0 | 302 | 11.0 | 36.4 | 5.1 | 6.0 | 5.0 | 320 | 91 | 240 | 320 |
| ScAlN1 | 2 | 804 | 1203 | 112.6 | 112.6 | 165 | 7.6 | 46.1 | 4.2 | 4.5 | 0.6 | 317 | 132 | 31 | 65 |
| ScAlN2 | 1 | 511 | 959 | 28.4 | 28.3 | 748 | 18.6 | 24.9 | 4.7 | 5.4 | 4.0 | 194 | 54 | 223 | 141 |
| ScAlN2 | 2 | 511 | 959 | 177.4 | 177.3 | 320 | 11.2 | 35.0 | 4.0 | 4.6 | 31.0 | 193 | 89 | 26 | 32 |
| ScAlN3 | 1 | 327 | 767 | 43.7 | 44.2 | 875 | 13.8 | 15.8 | 4.2 | 4.9 | 0.5 | 128 | 95 | 24 | 14 |
| ScAlN3 | 2 | 327 | 767 | 273.3 | 277.1 | 436 | 10.5 | 24.1 | 3.7 | 3.8 | 0.6 | 127 | 144 | 8 | 5 |
| ScAlN4 | 1 | 1000 | 1000 | 25.6 | 26.0 | 778 | 39.0 | 50.1 | 4.9 | 5.7 | 35.0 | 337 | 26 | 124 | 312 |
| ScAlN4 | 2 | 1000 | 1000 | 159.4 | 163.0 | 167 | 9.7 | 57.9 | 3.8 | 4.6 | 5.0 | 335 | 104 | 17 | 58 |
| AlN1 | 1 | 513 | 1602 | 10.6 | 11.1 | 660 | 8.2 | 12.4 | 2.6 | 2.6 | 41.2 | 138 | 122 | 1070 | 185 |
| AlN1 | 2 | 513 | 1602 | 70.7 | 69.8 | 532 | 10.7 | 20.1 | 2.3 | 2.5 | 4.7 | 127 | 94 | 112 | 45 |

In order to describe the cantilever deflection a model is employed as described for instance in Leighton *et al.* that assumes $T \ll w < L$, where L denotes the cantilever length, w the width and T the thickness [10]. It assumes that the actuation potential of the piezoelectric film upon application of an electric field E translates into an out-of plane bending moment M_{OP} . The total thickness T is the sum of the silicon device layer thickness t_b , the piezoelectric film thickness t_p and the electrode thickness t_{Et} . M_{OP} is proportional to the induced in-plane strain $\epsilon = V/t_p d_{31}$ which is extracted from the equation to yield $M_{OP}' = M_{OP}/\epsilon$. The deflection Δz at a position x along the cantilever length L is then given at the resonance frequency via a dynamic calculation as:

$$\Delta z(x) = d_{31} \frac{M'_{OP}}{m\omega_i^2} \phi'_{cf,i}(L) \phi_{cf,i}(x) QV \quad (1.1)$$

where ω_i is the Eigenfrequency, $\phi_{cf,i}$ the mode shape, $\phi'_{cf,i}$ its slope at the cantilever tip $x = L$ and the applied voltage V . The Q -factor appears due to the employed model that describes the dynamic form by a transfer function which has the absolute value Q at the resonance frequency.

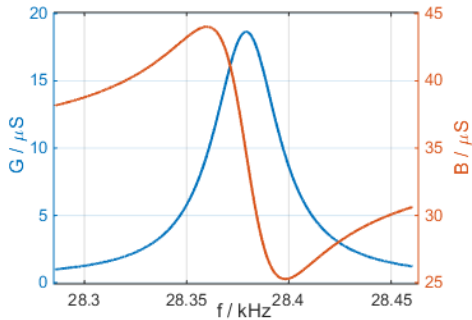


Figure 5: Conductance G and susceptance B near the 1_{st} out-of plane eigenmode of a ScAlN excited cantilever ($W = 511 \mu\text{m}$, $L = 959 \mu\text{m}$) in air.

Electrical Admittance

The dynamic response of the cantilever is measured electrically using an Agilent 4294A precision impedance analyser. In analogy to the measurements performed with the LDV, the top and bottom electrode pairs are excited in parallel to further study the OP eigenmodes. The conductance G and susceptance B are measured around each Eigenfrequency and a Butterworth Van Dyke equivalent circuit model is fitted to the frequency response as described in the work of Kucera *et al.* [2]. In addition to the equivalent circuit parameters, the conductance peak height ΔG and the Q -factor are extracted with this approach. A typical measurement of a ScAlN based cantilever design oscillating at resonance in the fundamental mode is shown in Figure 5. The described approach yields the following fitting results: $\Delta G = 18.6 \mu\text{S}$ and $Q = 748$. These parameters are further used to calculate the effective piezoelectric constant d_{31} . For this purpose, the conductance peak is calculated as being proportional to the dynamic capacitance change due to the induced piezoelectric charge. The derivation in analogy to Kucera *et al.*, but for OP modes yields for the conductance peak [2]:

$$\Delta G = d_{31}^2 \frac{M'_{OP}}{2\omega_i} \frac{E_p}{\rho L} \phi_{cf,i}^2(L) Q \quad (1.2)$$

with the in-plane modulus of ScAlN E_p , average density ρ and curve shape functions $\phi_{cf,i}$. For the evaluation $E_p = 327 \text{ GPa}$ and $E_p = 217 \text{ GPa}$ was considered for pure AlN and ScAlN, respectively [8].

RESULTS & DISCUSSION

Cantilevers in different geometric dimensions were fabricated and evaluated electrically and optically. Electrical admittance measurements were used to extract equivalent

BVD circuit parameters from a fitting procedure of the data around the corresponding eigenfrequency. The transversal piezoelectric coefficient d_{31} was calculated from conductance peak height and deflection maxima, respectively. For comparison purposes, a cantilever based on pure AlN is analyzed in addition to the ScAlN based devices. Table 1 gives an overview of the results for four different ScAlN based cantilevers and one excited with a pure AlN film. For each device, the first and second OP modes are evaluated. The piezoelectric constants from deflection and conductance measurements agree reasonable well. On average the ScAlN cantilever exhibit a d_{31} of $-(4.3 \pm 0.5)$ pm/V and $-(4.9 \pm 0.7)$ pm/V, respectively. Furthermore, evaluation of the reference AlN based cantilever yields an average $d_{31} = -2.5$ pm/V. Q-factors from deflection measurements match the electrically determined values closely. The signal level ΔG is clearly largest for the ScAlN cantilever having the largest electrode area as expected theoretically. Theoretically calculated values for the resonance frequencies are close to the measurements, with discrepancies explained by the atmospheric measurement conditions in addition to deviations from variations of sputtered thin film thickness across the wafer. Equivalent motional parameters for a series RLC are shown in table 1 in addition to R_p and C_p which describe the good quality of the fabricated devices in terms of parallel resistance due to leakage current and parasitic capacitance.

CONCLUSIONS

In this study, the fabrication of $\text{Sc}_x\text{Al}_{1-x}\text{N}$ ($x = 27\%$) based piezoelectric MEMS cantilevers was successfully demonstrated. For characterization, ScAlN thin films with 500 nm thickness are prepared via DC reactive sputter deposition. Patterning of the ScAlN layer is done with an ICP-RIE process based on SiCl_4 . This dry etching process is anisotropic and therefore, prevents due to the high physical character, underetching of the ScAlN thin film. Etch rates of about 10 nm/min were observed and improved etch recipes are currently investigated. The characterization employs measurements of the vertical deflection and analysis of the admittance. The frequency response of conductance and susceptance is fitted to a BVD equivalent circuit model. Further evaluation of the first two OP conductance peaks and the deflection peaks from LDV measurements yield $d_{31} = 4.3$ pm/V and $d_{31} = 4.9$ pm/V, respectively. Thus, the reported piezoelectric coefficients are significantly higher compared to values for pure AlN. Potential for further optimization of the ScAlN deposition process remains due to higher, reported d_{31} values for ScAlN on Si [8].

ACKNOWLEDGEMENTS

Reactive ion etching was partially performed at the centre for micro- and nanostructures (ZMNS) in Vienna. Patrick Meyer and Christopher Rehleendt are thanked for their help with device fabrication. For financial support we gratefully acknowledge the Austrian Science Fund (FWF), number P 25212-N30.

REFERENCES

- [1] J. Tamayo, P. M. Kosaka, J. J. Ruz, A. San Paulo, and M. Calleja, "Biosensors based on nanomechanical systems", *Chemical Society Reviews*, 42, 3 (2013), pp. 1287-1311.
- [2] M. Kucera, E. Wistrela, G. Pfusterschmied, V. Ruiz-Diez, T. Manzanique, J. Hernando-Garcia *et al.*, "Design-dependent performance of self-actuated and self-sensing piezoelectric-AlN cantilevers in liquid media oscillating in the fundamental in-plane bending mode", *Sensors and Actuators B-Chemical*, 200, (2014), pp. 235-244.
- [3] M. Akiyama, K. Umeda, A. Honda, and T. Nagase, "Influence of scandium concentration on power generation figure of merit of scandium aluminum nitride thin films", *Applied Physics Letters*, 102, 2 (2013), pp. 021915(1-4).
- [4] W. B. Wang, P. M. Mayrhofer, X. L. He, M. Gillinger, Z. Ye, X. Z. Wang *et al.*, "High performance AlScN thin film based surface acoustic wave devices with large electromechanical coupling coefficient", *Applied Physics Letters*, 105, 13 (2014), pp. 133502(1-4).
- [5] A. Teshigahara, K.-Y. Hashimoto, and M. Akiyama, "Scandium aluminum nitride: Highly piezoelectric thin film for RF SAW devices in multi GHz range". pp. 1-5.
- [6] M. Moreira, J. Bjurstrom, I. Katardjev, and V. Yantchev, "Aluminum scandium nitride thin-film bulk acoustic resonators for wide band applications", *Vacuum*, 86, 1 (2011), pp. 23-26.
- [7] K. Umeda, H. Kawai, A. Honda, M. Akiyama, T. Kato, and T. Fukura, "Piezoelectric Properties of ScAlN thin films for piezo-mems devices", 26th Ieee International Conference on Micro Electro Mechanical Systems (Mems 2013) (2013), pp. 733-736.
- [8] P. M. Mayrhofer, H. Euchner, A. Bittner, and U. Schmid, "Circular test structure for the determination of piezoelectric constants of $\text{Sc}_x\text{Al}_{1-x}\text{N}$ thin films applying Laser Doppler Vibrometry and FEM simulations", *Sensors and Actuators A: Physical*, 222, (2015), pp. 301-308.
- [9] F. A. Khan, L. Zhou, V. Kumar, I. Adesida, and R. Okojie, "High rate etching of AlN using $\text{BCl}_3/\text{Cl}_2/\text{Ar}$ inductively coupled plasma", *Materials Science and Engineering B-Solid State Materials for Advanced Technology*, 95, 1 (2002), pp. 51-54.
- [10] G. J. T. Leighton, P. B. Kirby, and C. H. J. Fox, "In-plane excitation of thin silicon cantilevers using piezoelectric thin films", *Applied Physics Letters*, 91, 18 (2007), pp. 183510(1-3).

CONTACT

*P.M. Mayrhofer, tel: +01-158801-76635;
patrick.mayrhofer@tuwien.ac.at